

Multifunctional Polyimides for Resistive Switching Memory Devices Based on Flexible Transparent Polyimide–AgNWs Hybrid Electrodes

Guoshu Liu¹, Jinghong Zhang¹, Zuxin She², Liangyi Peng³, Lunjun Qu¹, Kaiti Wang¹, Hailong Tang¹, and Chaolong Yang¹

¹Chongqing University of Technology

²Southwest Technology and Engineering Research Institute

³Sinopec Lubricant Co Chongqing Branch

November 7, 2022

Abstract

With the quick development of flexible memory electronics, multifunctional organic materials have been the necessary for fabricate electronics. In this work, the highly transparent and flexible electrode was successfully prepared by coating the high-performance silver nanowires (AgNWs) onto the colorless polyimide (PI) substrate. The prepared flexible PI-AgNWs electrodes exhibited a low sheet resistance of 15 Ω /sq with the high transparency of 68 % at the wavelength of 400 nm. A novel kind of polyimide TPC6FPI was successfully synthesized and characterized with excellent thermal stabilities and high glass transition temperature (T_g) above 250 °C. Furthermore, a kind of flexible transparent PI-AgNWs/ TPC6FPI/Al resistive memory device was prepared and exhibited excellent SRAM switching behavior with the threshold voltage of around 2.1V and the ON/OFF current ratio of $\sim 10^4$, which indicated that multifunctional PI-based memory device showed the potential to the wearable devices.

1 Introduction

Nowadays, flexible electronics are widely used in our daily lives because of their better convenience and providing us more bright horizons.^[1-2] With the rapid growth of digital information over the past decades, the traditional optical and magnetic storage technologies have almost reached their theoretical and physical limits, which cannot meet the huge demands of memory devices for high-density, fast response and flexible data storage.^[3-5] Compared with the traditional memory devices, resistive random-access memory (RRAM) devices with a top electrode/active layer/bottom electrode sandwiched structure^[6], play an important role in the next-generation digital memory devices due to their high performance, high reliability^[7], fast operation^[8], excellent scalability^[9] and durable flexibility^[10], and attract much attention as one of the most promising candidates such as the resistor, capacitor and transistor, etc.^[11-13] However, the performance of flexible RRAM devices still faces many challenges such as the serious degradation of reliability during continued deformation.

To meet the increasing requirement of flexible RRAM devices, polymers as the active layer are more favorable than other materials due to their low cost, intrinsic flexibility and large area fabricating capability.^[14-16] Polymer memory materials can store data through the conversion between the low and high current states between two electrodes by the applied voltage, which can be assigned as “0” and “1” or “OFF” state and “ON” state.^[17-21] In recent years, functional polyimides (PIs) are regarded as the most promising polymeric memory materials due to their excellent thermal resistance^[22], chemical stability^[23], mechanical durability^[24]

and flexibility^[25]. More importantly, PIs with the special donor-acceptor (D-A) type molecular structures exhibiting stronger intramolecular and intermolecular charge transfer (CT) effects are more promising for the flexible memory devices.^[26-29] Up to now, a large number of PIs exhibit various kinds of memory properties, including the volatile memory properties (Dynamic Random-Access Memory^[31] (DRAM), Static Random Access Memory^[32] (SRAM)) and the non-volatile memory properties (FLASH^[33], Write Once Read Many^[34] (WORM)). However, most reported PI based memory devices are rigid and non-wearable, which limits their application in flexible electronics.^[35]

In order to reach the demand of wearable intelligent electronic memory devices, advances in electrodes are essential to enhance the properties of both high conductivity, flexibility and transmittance. The polymer-based electrodes have attracted great attention by investigating indium tin oxide (ITO)^[36], carbon nanotubes (CNTs)^[37], graphene^[38], and metallic nanowires^[39], etc. Especially, silver nanowires (AgNWs) have been considered as the most potential candidates in the future.^[40-42] However, the poor adhesion properties of AgNWs and the lower glass transition temperature (T_g) of flexible substrates are further restricted to the development of the polymer-AgNWs electrodes.

Hence, in this work, we designed and synthesized a kind of thermally stable and colorless polyimide (PI) with a high T_g and high transmittance in the visible light area, which was chosen to prepare flexible PI-AgNWs hybrid electrodes. Then, a novel kind of polyimide memory material (TPC6FPI) was prepared by the polycondensation of the diamine 4,4'-((4-(diphenylamino)phenyl)methylene)dianiline (TPCDA) and the dihydride 2,2-bis(3,4-anhydrodicarboxyphenyl)-hexafluoropropane (6FDA), which was used for the flexible resistive memory device with a sandwich-like structure fabricated by casting TPC6FPI as active layers between the bottom PI-AgNWs hybrid electrodes and top Al electrodes. Furthermore, the performance of PI-based flexible memory devices exhibiting SRAM type memory behavior were systematically studied and evaluated. This study aimed to provide an effective and reliable method for the performance optimization of multifunctional flexible PI based memory devices.

2 EXPERIMENTAL

2.1 Synthesis of colorless PI

As shown in Figure 1a, the colorless polyimide TFBPI used in this work was synthesized according to a traditional two-step by thermal imidization as follows: 1.0410 g (2 mmol) of 4,4'-[(isopropylidene)bis(p-phenyleneoxy)]diphthalic dianhydride (BPADA) and 0.6404 g (2 mmol) of 2,2'-Bis-trifluoromethyl-biphenyl-4,4'-diamine (TFMB) were added into a solution of N,N-dimethylformamide (DMF) (20 wt% solid content) under a nitrogen (N_2) flow to react over 12 h to form polyamide acid (PAA) at room temperature. The resulting PAA solution was coating on a glass substrate to form TFBPI thin film by raising the temperature slowly to 300 °C to complete the thermal imidization.

2.2 Preparation of AgNWs

Silver nanowires were synthesized by the modified polyol process: 2 g of polyvinylpyrrolidone (PVP) was added into ethylene glycol and glycerol mixed solution (50 mL) stirred at 130 °C to dissolve under a N_2 flow. After cooling to the room temperature, 0.1 g of silver nitrate ($AgNO_3$) and (NaBr) 0.5 mL were added unto the reactor and stirred for 0.5 h. Finally, the mixed solution was moved into vacuum oven for an oxidation reaction over 6 h at 150 °C. The resulting AgNWs were obtained and washed by ethanol with centrifugation filtration 5 times to remove the residual PVP and silver nanoparticles.

2.3 Preparation of PI-AgNWs hybrid electrodes

The AgNWs were firstly transferred from ethanol to DMF by using a solvent exchange method. And the weight fraction of the AgNWs in DMF solution with 1.0 mg/mL was modulated through thermogravimetry analysis. Then, the AgNWs solutions were coated on the TFBPI substrates, and performed thermal annealing at 200 °C for 0.5 h under inert condition to decrease the electrical resistance of the PI- AgNWs hybrid electrodes.

2.4 Synthesis of TPC6FPI memory materials

The diamine TPCDA was synthesized according to our reported work^[16] with high efficiency, and the detail synthesis process (**Scheme S1**), structure characterization (**Figure S1**) and measurement method were detailed described in Supporting Information. TPC6FPI was prepared by the chemical imidization as follows: 0.2221 g (0.5 mmol) of 6FDA and 0.2206 g (0.5 mmol) of TPCDA were added into DMF solution (20 wt% solid content) to stirred for 12 h to form PAA solution. Then, acetic anhydride (1 mL) and triethylamine (0.5 mL) were added and the imidization reaction proceeded over 48 h at room temperature. The resulting polyimide solution was poured into 250 mL of ethanol giving a light-yellow precipitate, which was collected by filtration.

2.5 Fabrication of PI-AgNWs/TPC6FPI/Al memory device

The flexible memory device was fabricated on AgNWs-coated colorless PI with the configuration TFBPI-AgNWs/TPC6FPI/Al. The active layer was fabricated by spreading a 50 mg/mL TPC6FPI solution in DMF onto the TFBPI-AgNWs substrate using a spin coater set at 2000 rpm. the spin-coated films were thermally treated under vacuum at 150 °C for 1 h to remove the remaining solvent. The thickness of the TPC6FPI film was about 40 nm. Finally, the sandwich devices were fabricated by vacuum evaporation of a thin Al layer (ca. 200 nm) through a shadow mask onto the polymer surface as the top electrode.

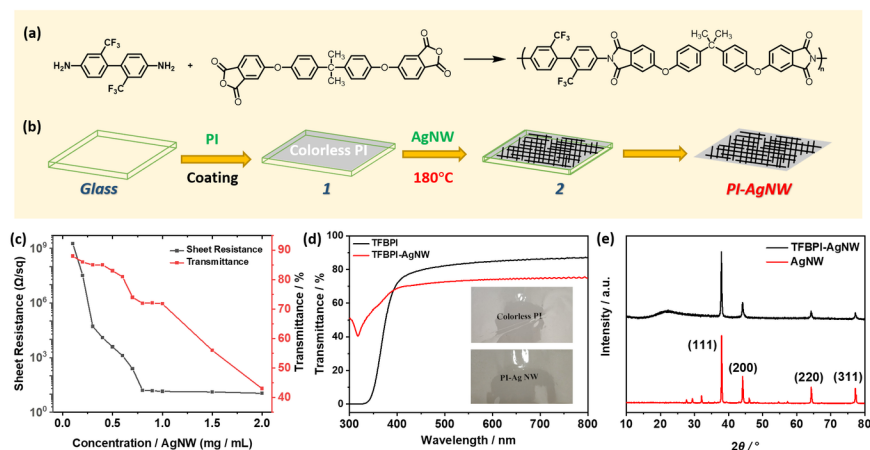


Figure 1 (a) The synthetic scheme for the synthesis of colorless polyimide TFBPI; (b) The scheme of the procedure for the transparent TFBPI-AgNWs hybrid electrodes; (c) Transmittance at 800 nm wavelength, sheet resistance of AgNWs suspension with different concentrations ranging from 0.1 mg/mL to 2.0 mg/mL; (d) UV-vis transmittance spectra of TFBPI and TFBPI-AgNWs; (e) The XRD pattern of AgNWs and TFBPI-AgNWs.

3 RESULTS AND DISCUSSION

3.1 Properties of the colorless TFBPI

The colorless TFBPI used as substrate materials in this work were shown in **Figure 1a** and characterized by FT-IR in **Figure S2**. The FT-IR characteristic peaks around 1780 cm^{-1} , 1715 cm^{-1} and 1370 cm^{-1} , were attributed to the imide groups. There were no peaks of amino groups at 3500 cm^{-1} appeared, which indicated TFBPI was imidized completely. The TFBPI exhibited excellent solubility in common organic solvents, such as DMF, DMSO and NMP, which provided an easy blending method with AgNWs. The TFBPI showed excellent thermal stabilities, and the diagrams of the thermogravimetric and thermomechanical analyses were depicted in **Figure S3** and **S4**, respectively. The 5 wt% decomposition temperatures ($T_{d5\%}$) and T_g values of TFBPI were 510 °C and 260 °C, indicating that the PI exhibited highly thermal stability. The

optical properties of TFBPI were investigated by ultraviolet-visible (UV-Vis) absorption and transmittance. The optical transmittance of TFBPI thin film at 400 nm is 76 % and the ultraviolet-visible cutoff wavelength of 80 % is 432 nm. And the maximum absorption at 306 nm and the edge absorption 341 nm, indicating the charge transfer effect depressed to result in a colorless TFBPI.

3.2 Properties of the TFBPI-AgNWs hybrid based transparent electrode

The scheme of the procedure and the transparency of the TFBPI-AgNWs hybrid electrodes was shown in **Figure 1b**. The AgNWs were prepared with a modified polyol process by the ethylene glycol and glycerol used as the reductant and solvent, the NaBr used as the oxygen scavenger and PVP used as the capping agent. The obtained PI-based flexible electrodes with different amounts of AgNWs were summarized in Figure 1c. With the increasing concentrations of AgNWs from 0.1 mg/mL to 2.0 mg/mL, the transmittance of PI-based flexible electrodes was cut down from 88 % to 42% at 800 nm. At the same time, the sheet resistance of flexible electrodes was decreased quickly from $\sim 10^9 \Omega/\text{sq}$ to $15 \Omega/\text{sq}$ at the concentrations of 1.0 mg/mL, which was comparable to the commercial ITO electrodes to meet the performance on flexible substrates for the resistive memory applications. As we all knew, it was rare difficult for flexible PI-AgNWs electrodes to achieve a high transmittance with low resistance simultaneously due to the dilemma relationship between transmittance and conductivity. Therefore, in this work, 1.0 mg/mL of AgNWs in DMF solution was chosen to prepare flexible TFBPI-AgNWs hybrid based transparent electrode. Compared to the TFBPI thin film, the transmittance of the TFBPI-AgNWs hybrids at 400 nm was down to 67 %, and the maximum transmittance was still beyond 70 %, as shown in **Figure 1d**. The inset image of TFBPI thin film and TFBPI-AgNW flexible electrode suggested the synthesized polyimide exhibited excellent transparency. And the XRD patterns of TFBPI-AgNW flexible electrode was similar with the AgNWs except for the wide dispersion peak of polyimide around 22° , which indicated that the cell structure of AgNWs was not changed by thermal annealing with high temperature.

The morphology of the AgNWs was measured by SEM and TEM, and these images were depicted in **Figure 2**. The obtained AgNWs had an average diameter around 50 nm and an average length of 30 nm, suggesting that the average aspect ratio of these AgNWs was around 600, which was high enough for the flexible transparent electrodes. And the selected area electron diffraction (SAED) image of AgNW indicated that the prepared electrode showed highly ordered lattice and interface. Therefore, the TFBPI-AgNW flexible electrode was prepared with high conductivity and transparency, which exhibited the potential application for the flexible electronics.

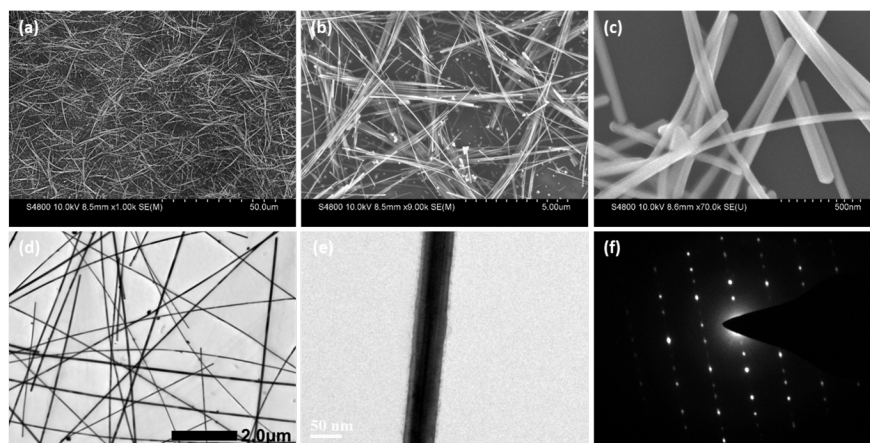


Figure 2 (a), (b) and (c) SEM images of the synthesized AgNWs with 1.0 mg/mL; (d) and (e) TEM images of the synthesized AgNWs with 1.0 mg/mL; (f) Selected area electron diffraction (SAED) image of AgNWs.

3.3 Properties of TPC6FPI memory materials

The polymer TPC6FPI was synthesized by chemical imidization, as shown in **Figure 3a**. TPC6FPI exhibited good solubility in a variety of polar solvent such as DMF and DMSO, and the intrinsic viscosities of TPC6FPI was of 0.82 dL/g. The high solubility was attributed to the introduction of bulky side-chain triphenylamine group in the polymer structure. The $T_{d5\%}$ and T_g values of TPC6FPI were 489 °C and 252 °C, respectively, as shown in **Figure 3b** and **3c**. The optical spectra of the TPC6FPI in thin film state and in DMF solution were shown in **Figure 3d**, **3e** and **3f**. TPC6FPI exhibited the absorption peak maxima at 266 nm in solution which was the assignable to the $\pi-\pi^*$ transition. And the middle absorption peak around 300 nm was belong to $n-\pi^*$ intramolecular charge transfer (CT) effect, which even showed the yellow color due to stronger the intermolecular CT effect in thin film state. Thus, the optical band gap of TPC6FPI was estimated to be 3.35 eV with the initial absorption wavelength at around 370 nm. The emission spectra of TPC6FPI in DMF solution was obtained with the maximum excitation wavelength of 393 nm. TPC6FPI exhibited intense emission peaks at 433 nm, consistent with the fact that the triphenylamine derivatives was efficient fluorescence chromophores.

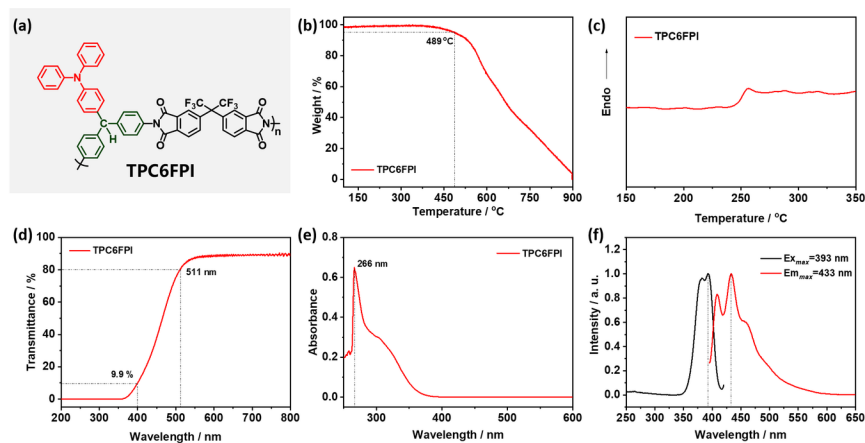


Figure 3 (a) Synthesis structure of TPC6FPI; (b) TGA curves and (c) DSC curves of TPC6FPI at a scan rate of 20 °C/min under N_2 ; (d) UV-vis. transmittance and (e) absorption spectra of TPC6FPI in thin film state and in DMF solution (10^{-5} M); (f) photoluminescence curves of TPC6FPI in DMF solution (10^{-5} M).

3.4 Memory device characteristics of PI-AgNWs/TPC6FPI/Al

The memory effects of TPC6FPI were demonstrated by the current–voltage (I–V) characteristics of a flexible PI-AgNWs/TPC6FPI/Al device. The PI-based memory device can store data based on the high (“ON” and low “OFF”) bistable conductive state responses to the external applied voltages.^[8,12,23] **Figure 4a** exhibited the typical I–V curves of the memory devices fabricated with TPC6FPI. The I–V characteristics were measured by scanning the voltage from 0 to ± 4 V. As shown in **Figure 4b**, initially, the device was in the OFF state (“0” signal in data storage) with a current in the range from $\sim 10^{-11}$ to $\sim 10^{-7}$ A with the voltage swept increasing from 0 V (sweep 1). When the voltage raised further, a sharp increase in current at a threshold voltage of about 2.1V, which indicated that the transition from the OFF state to the ON state (“1” signal in data storage) occurred current from $\sim 10^{-6}$ to $\sim 10^{-5}$ A. The electronic transition from the OFF state to the ON state was served as the “writing” process. Furthermore, the flexible device maintained the ON state under the positive voltage scan (sweep 2) from 4 V to 0, almost keeping the current curves on conductive state. After the applied voltage was turned off about 1 minutes, the device relaxed to the OFF state again. The memory device could be reset from the initial OFF state to ON state by the application of a reverse sweep (sweep 3) at -2.4 V. the following sweep from -4 V to 0V (sweep 4) was still stable at high conductivity. Therefore, the flexible PI-based memory device which kept the OFF and ON state was randomly accessible and volatile, which suggested that the resistive switching behavior was regarded as the static random-access memory (SRAM) characteristic.

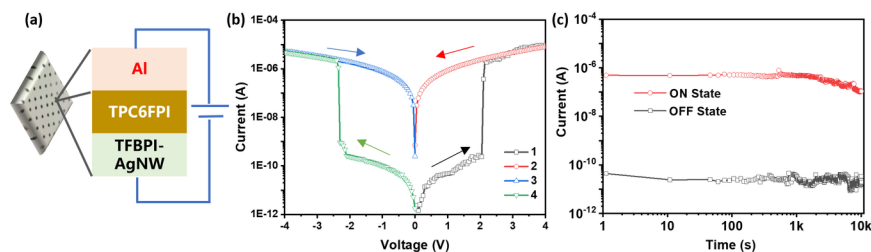


Figure 4 (a) Schematic diagram of the for the flexible PI-AgNWs/TPC6FPI/Al memory device; (b) Current–voltage (I–V) characteristics of the memory device with an electrode are of 0.25 mm^2 ; Retention characteristics of both ON and OFF states for the memory device under a constant stress (1.0 V) at room temperature.

The I-V characteristics were also found to have good reproducibility, except for the slight variations in switching threshold voltages associated with the sheet resistance of flexible PI-AgNWs electrodes, as shown in **Figure S6** and **S7**. In addition, the flexible memory device maintained an ON/OFF current ratio as high as 10^4 at 1 V, and the no obvious degradation in current density was observed for both the ON and OFF states over a 2 h period (**Figure 4c**).

Furthermore, the charge transport mechanism could be obtained from the I–V curves in OFF and ON states according to the reported various conduction models in the literature. As shown in **Figure 5a**, the OFF states for the PI-AgNWs/TPC6FPI/Al device exhibited the space charge limited current model^[6] (SCLC, from 0 to 2.0 V), which was described by the equation as follow: $I = 9A\epsilon\epsilon_0\mu V^2/8d^3$, where d was thickness of active layer, μ was the carrier mobility of polymer, $\epsilon\epsilon_0$ was the absolute dielectric constant. On the other hand, as shown in **Figure 5b**, the current in the ON state was almost linear in dependence on applied voltage just as the ohmic model^[23], which indicated that the ON state the charge transport dominated similarly as metallic conduction.

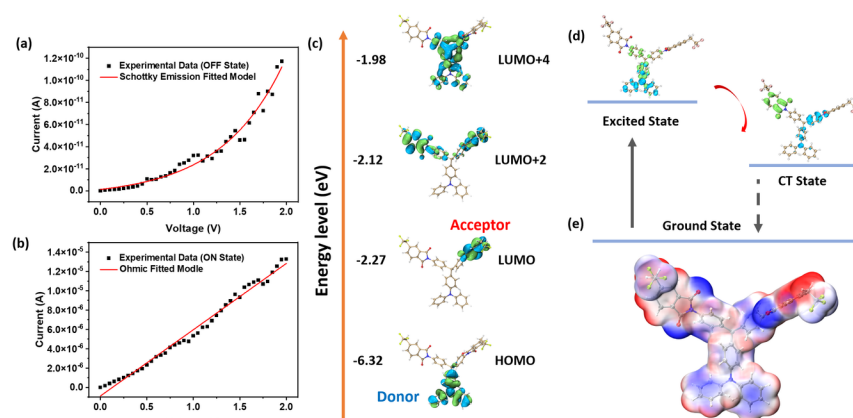


Figure 5 (a) Experimental and fitted data of I–V curves for the memory devices in the OFF states with the SCLC model; (b) Experimental and fitted data of I–V curves for the memory devices in the ON states with the ohmic current model; (c) Calculated molecular orbitals (isovalue=0.05) and (d) the plausible electronic transition processes occurred on TPC6FPI (Note: Blue and green isosurfaces represent hole and electron distributions, respectively); (e) Electrostatic potential (ESP) surface of TPC6FPI.

The above results suggested that the bipolar ON and OFF switching behaviors of TPC6FPI film could be

simulated well according to proper theoretical model. Geometry optimization of TPC6FPI was realized by DFT with dispersion-corrected density functional theory (DFT-D3) at the B3LYP-D3/def2-SVP level, and their excitation energies were calculated at the CAM-B3LYP/def2-SVP level with TD-DFT method.^[43-44] The detail progress of calculation was described in the Supporting Information. As shown in **Figure 5c**, the highest occupied molecular orbital (HOMO) and HOMO+4 mainly located on the triphenylamine unit, which was the donor cell of the structure of TPC6FPI. While the lowest unoccupied molecular orbital (LUMO) and the LUMO+2 distributed on the phthalimide unit completely, which was the acceptor cell of the structure of TPC6FPI. It was noted that the switching behavior between the OFF state and ON state correspond to electronic transition from the ground state to the excited state. The electron was easily excited from the HOMO to LUMO+4 by the applied bias reaches at the threshold voltage. However, the excited state tended to relax to LUMO by internal conversion leading to the forming the charge transfer (CT) effect. The charge-transfer (CT) complex was beneficial to stable the ON state. After the applied voltage was turned off, the charge-transfer (CT) complex was slowly returned to the initial state. This progress was described in **Figure 5d** by the hole-electron analysis to fully characterize electron excitations. It was noted that blue and green isosurfaces represent hole and electron distributions, respectively.^[45] As shown in **Figure 5e**, The Electrostatic potential (ESP) surfaces showed that TPC6FPI consisted mainly of the positive ESP region (red color)^[46], with special independent negative regions (blue color) mainly arising from the sp² hybridized O atoms in the phthalimide unit. These negative ESP regions suggested that concentrated local electron densities near the phthalimide group possessed a certain electron-withdrawing ability, suggesting that electrons would be transferred from the triphenylamine moiety to the phthalimide moieties under excitation. Therefore, the separation of hole and electron was easy to form a charge transfer excited state, which was the characteristic of the structure of polyimide. In other word, the strong charge transfer effect of polyimides was the essence of resistive switching memory device.

4 Conclusion

In conclusion, introducing the prepared the AgNWs on to colorless PI through a facile solution casting method was demonstrated as an effective way to prepare flexible transparent electrodes in this work. The resulting flexible PI-AgNWs hybrid electrodes exhibited high transparency and high electrical conductivity with the sheet resistance of 15 Ω /sq. In addition, the multifunctional polyimide TPC6FPI was synthesized and proved as a novel kind of memory materials. The PI-AgNWs/TPC6FPI/Al resistive memory device was successfully prepared and exhibited excellent SRAM switch behavior, which indicating that the flexible transparency PI-AgNWs hybrid electrodes afforded the potential to resistive switching memory devices and served as the electrodes for wearable devices.

Supporting Information

The supporting information for this article is available on the WWW under <https://doi.org/10.1002/eng2.xxxxx>.

Acknowledgement

The authors are grateful for the financial supports by the National Natural Science Foundation of China (Grant No. 52003032 and 22275025), the Science and Technology Research Program of Chongqing Municipal Education Commission (KJQN202001103, KJQN202101106 and KJQN202001104), the Natural Science Foundation of Chongqing (cstc2020jcyj-msxmX0312 and cstc2020jcyj-msxmX0556), Innovation Research Group at Institutions of Higher Education in Chongqing (CXQT19027) and Scientific Research Foundation for Chongqing University of Technology (2019ZD106).

CONFLICT OF INTEREST

The authors declare no conflict of interest

References

1. Zhang D, Huang T, Duan L. Emerging self-emissive technologies for flexible displays. **Advanced**

- Materials** **2020** , 32(15): 1902391.
2. Liu YF, Feng J, Bi YG, Yin D, Sun HB. Recent developments in flexible organic light-emitting devices. **Advanced Materials Technologies** **2019** , 4(1): 1800371.
 3. Kurosawa T, Higashihara T, Ueda M. Polyimide memory: a pithy guideline for future applications. **Polymer Chemistry** **2013** , 4(1): 16-30.
 4. Xu R-P, Li Y-Q, Tang J-X. Recent advances in flexible organic light-emitting diodes. **Journal of Materials Chemistry C** **2016** , 4(39): 9116-9142.
 5. Tsai C-L, Yen H-J, Liou G-S. Highly transparent polyimide hybrids for optoelectronic applications. **Reactive and Functional Polymers****2016** , 108: 2-30.
 6. Gao S, Yi X, Shang J, Liu G, Li R-W. Organic and hybrid resistive switching materials and devices. **Chemical Society Reviews****2019** , 48(6): 1531-1565.
 7. Chen Q, Wang Z, Lin M, Qi X, Yu Z, Wu L, et al. Homogeneous 3D vertical integration of parylene-C based organic flexible resistive memory on standard CMOS platform. **Advanced Electronic Materials** **2021** , 7(2): 2000864.
 8. Gao JY, Chen CK, Lin YC, Kuo CC, Chen WC. Highly Thermal Stable Polyimides Applied in Flexible Resistive Memory. **Macromolecular Materials and Engineering** **2021** , 306(12): 2100512.
 9. Liaw D-J, Wang K-L, Huang Y-C, Lee K-R, Lai J-Y, Ha C-S. Advanced polyimide materials: Syntheses, physical properties and applications. **Progress in Polymer Science** **2012** , 37(7):907-974.
 10. Xiong H, Ling S, Li Y, Duan F, Zhu H, Lu S, et al. Flexible and recyclable bio-based transient resistive memory enabled by self-healing polyimine membrane. **Journal of Colloid and Interface Science** **2022** , 608: 1126-1134.
 11. Lian L, Xi X, Dong D, He G. Highly conductive silver nanowire transparent electrode by selective welding for organic light emitting diode. **Organic Electronics** **2018** , 60: 9-15.
 12. Liu X, Ren S, Li Z, Guo J, Yi S, Yang Z, et al. Flexible Transparent High-Efficiency Photoelectric Perovskite Resistive Switching Memory. **Advanced Functional Materials** **2022** : 2202951.
 13. Spechler JA, Koh TW, Herb JT, Rand BP, Arnold CB. A transparent, smooth, thermally robust, conductive polyimide for flexible electronics. **Advanced Functional Materials** **2015** , 25(48): 7428-7434.
 14. Sun B, Li X, Feng T, Cai S, Chen T, Zhu C, et al. Resistive switching memory performance of two-dimensional polyimide covalent organic framework films. **ACS applied materials & interfaces****2020** , 12(46): 51837-51845.
 15. Kim JW, Lee SJ, Choi MY, Chang J-H. Colorless and Transparent Polyimide Microporous Film with Excellent Physicochemical Property. **Polymers** **2021** , 13(8): 1298.
 16. Qu L-j, Tang L-s, Liu S-w, Chi Z-g, Chen X-d, Zhang Y, et al. Preparation and photoluminescent properties of polyimides containing triphenylamine pendant group. **Acta Polym Sin** **2018** , 11: 1430-1441.
 17. Neese, F.; Wennmohs, F.; Becker, U.; Riplinger, C., The ORCA quantum chemistry program package. **Journal of Chemical Physics** **2020** , 152 (22), 224108
 18. Wang Y, Liu Y, Wang T, Liu S, Chen Z, Duan S. Low-temperature nanowelding silver nanowire hybrid flexible transparent conductive film for green light OLED devices. **Nanotechnology** **2022** , 33(45): 455201.
 19. Choi J-Y, Lee J, Jeon J, Im J, Jang J, Jin S-W, et al. High-performance non-volatile resistive switching memory based on a polyimide/graphene oxide nanocomposite. **Polymer Chemistry****2020** , 11(48): 7685-7695.
 20. Lee SJ, Choi MY, Kwac LK, Kim HG, Chang J-H. Comparison of Properties of Colorless and Transparent Polyimide Nanocomposites Containing Chemically Modified Nanofillers: Functionalized-Graphene and Organoclay. **Polymers** **2022** , 14(12): 2469.
 21. Qu L, Tang L, Bei R, Zhao J, Chi Z, Liu S, et al. Flexible multifunctional aromatic polyimide film: highly efficient photoluminescence, resistive switching characteristic, and electroluminescence. **ACS Applied Materials & Interfaces** **2018** , 10(14): 11430-11435.
 22. Tian Y, Zhu S, Di Y, Liu H, Yao H, Zhang Y, et al. HOMO-controlled donor-acceptor contained

- polyimide for nonvolatile resistive memory device. **Dyes Pigments** **2021** , 186: 109020.
23. An H, Ge Y, Li M, Kim TW. Storage mechanisms of polyimide-molybdenum disulfide quantum dot based, highly stable, write-once-read-many-times memristive devices. **Advanced Electronic Materials** **2021** , 7(1): 2000593.
 24. Zhang H, Zhou Y, Wang C, Wang S. Realizing the Conversion of Resistive Switching Behavior from Binary to Ternary by Adjusting the Charge Traps in the Polymers. **ACS Applied Electronic Materials** **2021** , 3(6): 2807-2817.
 25. Kim Y, Song S, Liaw D-J, Huang Y-C, Ko Y-G, Ihm K, *et al.* Digital memory characteristics of aromatic polyimides based on pyridine and its derivatives. **ACS Omega** **2018** , 3(10): 13036-13044.
 26. Chen K, Yin Y, Song C, Liu Z, Wang X, Wu Y, *et al.* Two-dimensional triphenylamine-based polymers for ultrastable volatile memory with ultrahigh on/off ratio. **Polymer** **2021** , 230: 124076.
 27. Oh J, Yoon SM. Resistive Memory Devices Based on Reticular Materials for Electrical Information Storage. **ACS Applied Materials & Interfaces** **2021** , 13(48): 56777-56792.
 28. Chen FY, Gao Y, Zhu YL, Hu KT, Nan JY, Shen YZ. Tristable Memory Devices Based on Soluble Polyimides Containing Pendant Carbazole and Phenyl Groups. **ChemistrySelect** **2022** , 7(28): e202200718.
 29. Liu Y, Zhou Z, Qu L, Zou B, Chen Z, Zhang Y, *et al.* Exceptionally thermostable and soluble aromatic polyimides with special characteristics: intrinsic ultralow dielectric constant, static random access memory behaviors, transparency and fluorescence. **Mater Chem Front** **2017** , 1(2): 326-337.
 30. Wang W, Zhou G, Wang Y, Yan B, Sun B, Duan S, *et al.* Multiphotoconductance Levels of the Organic Semiconductor of Polyimide-Based Memristor Induced by Interface Charges. **The Journal of Physical Chemistry Letters** **2022** , 13: 9941-9949.
 31. Chatterjee D, Jadhav UA, Javaregowda BH, Dongale TD, Patil PS, Wadgaonkar PP. Partially bio-based triarylamine-containing polyimides: Synthesis, characterization and evaluation in non-volatile memory device applications. **European Polymer Journal** **2021** , 147: 110327.
 32. Qu L, Huang S, Zhang Y, Chi Z, Liu S, Chen X, *et al.* Multifunctional polyimides containing tetraphenyl fluorene moieties: fluorescence and resistive switching behaviors. **Journal of Materials Chemistry C** **2017** , 5(26): 6457-6466.
 33. Yu H, Liu H, Tan H, Yao H, Song Y, Zhu S, *et al.* Inserting phenylethynyl linker into triphenylamine-based hyperbranched polyimide for effectively tuning memory performance. **Dyes Pigments** **2018** , 158: 97-103.
 34. Liu Y-W, Tang L-S, Qu L-J, Liu S-W, Chi Z-G, Zhang Y, *et al.* Synthesis and properties of high-performance functional polyimides containing rigid nonplanar conjugated fluorene moieties. **Chinese Journal of Polymer Science** **2019** , 37(4): 416-427.
 35. Zheng W, Yang T, Qu L, Liang X, Liu C, Qian C, *et al.* Temperature resistant amorphous polyimides with high intrinsic permittivity for electronic applications. **Chemical Engineering Journal** **2022** , 436: 135060.
 36. Peng W, Lei H, Qiu L, Bao F, Huang M. Perfluorocyclobutyl-containing transparent polyimides with low dielectric constant and low dielectric loss. **Polymer Chemistry** **2022** , 13(26): 3949-3955.
 37. Wang S, Liang Y, Zhuo W, Lei H, Javed MS, Liu B, *et al.* Freestanding polypyrrole/carbon nanotube electrodes with high mass loading for robust flexible supercapacitors. **Mater Chem Front** **2021** , 5(3): 1324-1329.
 38. Lee Y-G, Lee J. Free-standing manganese oxide on flexible graphene films as advanced electrodes for stable, high energy-density solid-state zinc-ion batteries. **Chemical Engineering Journal** **2021** , 414: 128916.
 39. Lu X, Zhang Y, Zheng Z. Metal-Based Flexible Transparent Electrodes: Challenges and Recent Advances. **Advanced Electronic Materials** **2021** , 7(5): 2001121.
 40. Lu H-Y, Chou C-Y, Wu J-H, Lin J-J, Liou G-S. Highly transparent and flexible polyimide-AgNW hybrid electrodes with excellent thermal stability for electrochromic applications and defogging devices. **Journal of Materials Chemistry C** **2015** , 3(15): 3629-3635.
 41. Wang Y, Chen Q, Zhang G, Xiao C, Wei Y, Li W. Ultrathin Flexible Transparent Composite Electrode

- via Semi-embedding Silver Nanowires in a Colorless Polyimide for High-Performance Ultraflexible Organic Solar Cells. **ACS Applied Materials & Interfaces** **2022** , 14(4): 5699-5708.
42. Li F-W, Yen T-C, Manavalan S, Liou G-S. Electroactive Triphenylamine-Based Polymer Films as Passivation Layers for Improving Electrochemical Oxidation Stability of Silver Nanowires. **ACS Applied Polymer Materials** **2021** , 3(6): 2971-2978.
 43. Weigend, F.; Ahlrichs, R., Balanced basis sets of split valence, triple zeta valence and quadruple zeta valence quality for H to Rn: Design and assessment of accuracy. **Physical Chemistry Chemical Physics** **2005** , 7 (18), 3297-3305.
 44. Yanai, T.; Tew, D. P.; Handy, N. C., A new hybrid exchange-correlation functional using the Coulomb-attenuating method (CAM-B3LYP). **Chemical Physics Letters** **2004** , 393 (1-3), 51-57.
 45. Lu, T.; Chen, F. W., Multiwfn: A multifunctional wavefunction analyzer. **Journal of Computational Chemistry** **2012** , 33 (5), 580-592.
 46. Humphrey, W.; Dalke, A.; Schulten, K., VMD: Visual molecular dynamics. **Journal of Molecular Graphics & Modelling** **1996** , 14 (1), 33-38.